



## ON THE LOCAL INTERACTION SIMULATION APPROACH (LISA) WITH APPLICATION TO LAYERED PLATES

Rodica IOAN<sup>\*\*\*</sup>, Veturia CHIROIU<sup>\*\*</sup>, Dinel POPA<sup>\*\*\*</sup>

<sup>\*</sup> University Spiru Haret, Bucharest

<sup>\*\*</sup> Institute of Solid Mechanics, Romanian Academy

<sup>\*\*\*</sup> University of Pitesti, Romania

Corresponding author: Rodica Ioan, E-mail: [rodicaioan08@yahoo.com](mailto:rodicaioan08@yahoo.com)

**Abstract** This article discusses the local interaction simulation approach (LISA) for simulation of wave propagation in inhomogeneous media such as the layered plates. The method is applied to study the ultrasonic wave propagation in materials of arbitrary complexity and to solve some inverse problems of their characterization

*Key words:* Wave propagation, LISA, inhomogeneous media.

### 1. INTRODUCTION

Delsanto *et al.* have introduced in [1], [2] a method named *the local interaction simulation approach* (LISA) for simulation the propagation of ultrasonic wave in layered materials. The layered material is discretized in cells, each cell being associated to a layer with different mechanical properties. Each cell is put into a one-to-one correspondence to a processor of a parallel computer [3, 5]. The material properties are assigned as initial data to each processor. LISA aims *to teach* processors how the corresponding cells react to the arriving wave and propagate it to the neighbors by using a special interaction mechanism. LISA is efficient and flexible, especially in conjunction with parallel processing [6-10].

To explain the method, let us start with one-dimensional case, i.e. a layered plate with  $N$  homogeneous layers, each layer having the thickness  $h_n$ ,  $n = 1, 2, \dots, N$  [1]. The total thickness of

the plate is  $h = \sum_{n=1}^N h_n$ . The mathematical model is based on the assumption that an ultrasonic

longitudinal wave is transmitted through the plate, normal to its surface. Let us consider the case of a homogeneous, unstressed and isotropic single layer. The  $x$ -axis is in the direction of wave propagation, and  $x = 0$  and  $x = h$  represent two opposite surfaces of the plate.

The equation of longitudinal elastic wave  $u(x, t)$  is

$$(\lambda + 2\mu)u_{,xx} = \rho \ddot{u}, \quad (1)$$

where indexes represent the differentiation with respect to spatial coordinate, the superposed point means differentiation with respect to time,  $u$  is the longitudinal displacement,  $\lambda, \mu$  are the Lamé elastic constants, and  $\rho$  is the material density. Let us proceed to define a grid in time and space. We note by  $\delta$  the elementary time unit, so that the continuous time becomes  $t\delta$ ,  $t = 0, 1, 2, \dots$

The propagation path is divided into  $N$  cells of length  $\varepsilon = \frac{h}{N}$ . Consequently, we have  $(t, x) \rightarrow (T_i, X_i) = (t\delta, \varepsilon h)$ ,  $t = 0, 1, 2, \dots$ . The nod points between cells are label with indices  $i$ , such that  $i = 1$  corresponds to  $x = 0$ , and  $i = N + 1$  to  $x = h$ , respectively. The index  $i = 0$  is reserved for the input of the source pulse

$$u_0(t) = u_{\text{source}}(t). \quad (2)$$

Here,  $u_{i,t}$  is the value of  $u(x, t)$  in the point  $(T_i, X_i)$

$$u_{0,t} = u_0(t).$$

The finite difference (FD) method plays an important role in solving differential equations. The Taylor expansion of a differentiable function  $f(x)$

$$f(x + \varepsilon) = f(x) + \frac{\varepsilon}{1!} f'(x) + \frac{\varepsilon^2}{2!} f''(x) + \dots + \frac{\varepsilon^n}{n!} f^{(n)}(x) + \dots,$$

allows to extract the derivatives of different order by neglecting the terms in  $\varepsilon^2$  and higher as

$$f'(x) \cong \frac{f(x+h) - f(x)}{h}, \quad f'(x) \cong \frac{f(x+\varepsilon) - f(x-\varepsilon)}{2\varepsilon}. \quad (3)$$

For example, for ordinary differential equation  $y'(x) = ay(x) + b$ , the Euler method uses the finite difference (3) and the finite-difference equation can be written as  $y(x+h) = y(x) + h(ay(x) + b)$ . The error between the approximate solution and the true solution is determined by the error that is made by going from a differential operator to a difference operator. The *truncation error* reflects the fact that a difference operator can be viewed as a finite part of the infinite Taylor series of the differential operator.

Equation (1) may be written in finite-differences

$$u_{i,t+1} = c(u_{i-1,t} + u_{i+1,t}) + 2(1-c)u_{i,t} - u_{i,t-1}, \quad (4)$$

where the Courant constant  $c$  is a free parameter

$$c = \left( \frac{v_L}{v_c} \right)^2, \quad v_L^2 = \frac{\lambda + 2\mu}{\rho}, \quad v_c = \frac{\varepsilon}{\delta}, \quad (5)$$

where  $v_L$  is the longitudinal velocity and  $v_c$  is the cell characteristic velocity. From the theory of finite differential equations we know that the best choice, to achieve a complete stability, is  $c = 1$ . In this case, the waves are propagating without any degradation. The iteration equation (4) becomes

$$u_{i,t+1} = u_{i+1,t} + u_{i-1,t} - u_{i,t-1}. \quad (6)$$

This equation ensures that the wave keeps motion without any alteration, with a complete cancellation of the neglected higher order terms. Indeed, if the waves travel forward we have  $u_{i+1,t} = u_{i,t-1}$  from which it follows from (6) that  $u_{i,t+1} = u_{i-1,t}$ . For  $c < 1$ , numerical errors begin to accumulate and propagate, so that the method works only for a limited number of time steps. If  $c > 1$  the divergence in the displacement amplitudes is observed. From (6), an analogous iteration equation for stresses  $\sigma = (\lambda + 2\mu)u_{,x}$  is obtained

$$\sigma_{i,t+1} = \sigma_{i+1,t} + \sigma_{i-1,t} - \sigma_{i,t-1}. \quad (7)$$

The stresses from previously calculated displacement are calculated from  $\sigma_{i,t} = \frac{(\lambda + 2\mu)(u_{i+1,t} - u_{i,t})}{\varepsilon}$ , where the index  $i$  labels the cells for the stresses and the node-points for the displacements.

Each layer  $n$ , of length  $h_n$  it is divided in  $N_n$  cells of length  $\varepsilon_n = \frac{h_n}{N_n}$ ,  $N = \sum N_n$ . We choose  $\varepsilon_n$  so that

$$\varepsilon_n / \delta \geq \sqrt{\frac{\lambda_n + 2\mu_n}{\rho_n}}. \quad (8)$$

The interface between the first two layers is marked with  $i = N_1 + 1$ , and the interface between layers  $j$  and  $j + 1$ , with  $i = N_j + 1$ . For writing the recurrence relations at the interface between two layers of acoustic impedances  $Z_n$  and  $Z_{n+1}$  ( $Z_n = \rho_n \sqrt{\frac{\lambda_n + 2\mu_n}{\rho_n}} = S_n \sqrt{\frac{\rho_n}{\lambda_n + 2\mu_n}}$ ) we consider two points P and Q infinitely close to the interface, located on either side of it. At these points we impose the conditions of continuity of displacements and stresses

$$(\ddot{u})_P = (\ddot{u})_Q = (\ddot{u})_I, \quad \tau_P = (\lambda_1 + 2\mu_1)u'_P = \tau_Q = (\lambda_2 + 2\mu_2)u'_Q, \quad (9)$$

and have

$$(\lambda_1 + 2\mu_1) \left( 2 \frac{u_{I-1} - u_I}{\varepsilon_1^2} + 2 \frac{u'_P}{\varepsilon_1} \right) = \rho_1 \ddot{u}_I, \quad (10)$$

$$(\lambda_2 + 2\mu_2) \left( 2 \frac{u_{I-1} - u_I}{\varepsilon_2^2} + 2 \frac{u'_P}{\varepsilon_2} \right) = \rho_2 \ddot{u}_I. \quad (11)$$

By adding relations (10) and (11) we have

$$\frac{2(\lambda_1 + 2\mu_1)\delta^2}{\varepsilon_1(\varepsilon_1\rho_1 + \varepsilon_2\rho_2)}(u_{I-1} - u_I) + \frac{2(\lambda_2 + 2\mu_2)\delta^2}{\varepsilon_2(\varepsilon_1\rho_1 + \varepsilon_2\rho_2)}(u_{I-1} - u_I) = u_{t+1,I} - 2u_{t,I} + u_{t-1,I}, \quad (12)$$

where the recurrence relations results from the two-layer interface

$$w_{I,t+1} = t_I'' w_{I+1} + t_I' w_{I-1} + t_I w_I - w_{I,t-1}, \quad (13)$$

with

$$t_I'' = \frac{2(\lambda_1 + 2\mu_1)\delta^2}{\varepsilon_1(\varepsilon_1\rho_1 + \varepsilon_2\rho_2)} \quad t_I' = \frac{2(\lambda_2 + 2\mu_2)\delta^2}{\varepsilon_2(\varepsilon_1\rho_1 + \varepsilon_2\rho_2)} \quad t_I = 2 - t_I'' - t_I'. \quad (14)$$

When  $v_{c_n} = \varepsilon_n / \delta = v_{l_n} = \sqrt{(\lambda_n + 2\mu_n) / \rho_n}$  for each layer, then (10) and (11) are

$$(\lambda_1 + 2\mu_1) \left( 2 \frac{u_{I-1} - u_I}{\varepsilon_1^2} + 2 \frac{u'_P}{\varepsilon_1} \right) = \rho_1 \ddot{u}_I = \frac{Z_1 \delta}{\varepsilon_1} \cdot \frac{u_{t+1} - 2u_t + u_{t-1}}{\delta^2}, \quad (15)$$

$$(\lambda_2 + 2\mu_2) \left( 2 \frac{w_{I+1} - w_I}{\varepsilon_2^2} - 2 \frac{w_Q'}{\varepsilon_2} \right) = \rho_2 \ddot{w}_I = \frac{Z_2 \delta}{\varepsilon_2} \cdot \frac{w_{I+1} - 2w + w_{I-1}}{\delta^2}, \quad (16)$$

$$2Z_1(u_{I-1} - u_I) + 2Z_2(u_{I+1} - u_I) = (Z_1 + Z_2)(u_{I+1} - 2u + u_{I-1}), \quad (17)$$

where the recurrence relations results from the two-layer interface

$$w_{I,t+1} = t_I' w_{I+1} + t_I w_{I-1} - w_{I,t-1}, \quad (18)$$

in which the indices  $i, j, t$  were omitted.

The transmission coefficients in both directions  $t_I$  and  $t_I'$  are given by

$$t_I' = \frac{2Z_2}{Z_1 + Z_2} = \frac{2\zeta}{1 + \zeta} = 1 - r_I, \quad (19)$$

$$t_I = \frac{2Z_1}{Z_1 + Z_2} = \frac{2}{1 + \zeta} = 1 + r_I, \quad (20)$$

where  $r_I$  is the coefficient of reflection at the interface between two layers, and  $\zeta$  is the ratio of acoustic impedances

$$r_I = \frac{1 - \zeta}{1 + \zeta}, \zeta = \frac{Z_2}{Z_1}. \quad (21)$$

If  $\varepsilon_n = ct = \varepsilon$ , coefficients  $t_I$ ,  $t_I'$  and  $t_I''$  from (13) become

$$t_I'' = \frac{2(\lambda_1 + 2\mu_1)\delta^2}{\varepsilon_1(\varepsilon_1\rho_1 + \varepsilon_2\rho_2)}, \quad t_I' = (\lambda_2 + 2\mu_2) \frac{\delta^2}{\varepsilon^2} \left( \frac{\rho_1 + \rho_2}{2} \right), \quad t_I = 2 - t_I'' - t_I'. \quad (22)$$

## 2. THE BIDIMENSIONAL CASE

For bi-dimensional case, the wave propagation equation for isotropic media is given by [2]

$$(\lambda + \mu)w_{j,ji} + \mu w_{i,jj} = \rho \ddot{w}_i, \quad (23)$$

and can be written for this two-dimensional case under the form

$$AW_{,11} + BW_{,22} + CW_{,12} = \rho \ddot{W}, \quad (24)$$

where

$$A = \begin{pmatrix} \lambda + 2\mu & 0 \\ 0 & \mu \end{pmatrix}, \quad B = \begin{pmatrix} \mu & 0 \\ 0 & \lambda + 2\mu \end{pmatrix}, \quad C = \begin{pmatrix} 0 & \lambda + \mu \\ \lambda + \mu & 0 \end{pmatrix}, \quad W = \begin{pmatrix} w_1 \\ w_2 \end{pmatrix}. \quad (25)$$

With the finite difference method with a spatial mesh grid  $N_1 \times N_2$  of rectangular cells of size  $\varepsilon_1 \times \varepsilon_2$ , and a time discretization with the step  $\delta$ , for each point of the grid the displacements at  $t + 1$  in the case of no attenuation are

$$\begin{aligned}
W_{t+1,i,j} = & 2W_{t,i,j} - W_{t-1,i,j} + \delta^2 \left[ \frac{A}{\varepsilon_1^2} (W_{t,i+1,j} + W_{t,i-1,j} - 2W_{t,i,j}) + \right. \\
& \left. + \frac{B}{\varepsilon_2^2} (W_{t,i,j+1} + W_{t,i,j-1} - 2W_{t,i,j}) + \frac{C}{4\varepsilon_1\varepsilon_2} (W_{t,i+1,j+1} + W_{t,i-1,j-1} - W_{t,i-1,j+1} - W_{t,i+1,j-1}) \right].
\end{aligned} \quad (26)$$

Using the notations from Fig. 1, we get

$$\alpha_k = \frac{\delta^2(\lambda + 2\mu)}{\rho\varepsilon_k^2}, \quad k=1,2, \quad \beta_k = \frac{\delta^2\mu}{\rho\varepsilon_h^2}, \quad k=1,2, \quad h=3-k, \quad \gamma = \frac{\lambda + \mu}{4\rho\varepsilon_1\varepsilon_2}, \quad (27)$$

and omitting index writing  $t$ ,  $i$  and  $j$  we have

$$\begin{aligned}
u_{t+1} = & \alpha_1(u_5 + u_7) + \beta_1(u_6 + u_8) - 2(\alpha_1 + \beta_1 - 1)u + \gamma(v_1 - v_2 + v_3 - v_4) - u_{t-1}, \\
v_{t+1} = & \alpha_2(v_6 + v_8) + \beta_2(v_5 + v_7) - 2(\alpha_2 + \beta_2 - 1)v + \gamma(u_1 - u_2 + u_3 - u_4) - v_{t-1},
\end{aligned} \quad (28)$$

with  $u = w_1, v = w_2$ .

In isotropic materials we have  $\lambda + 2\mu = \rho c_p^2$  și  $\mu = \rho c_T^2$ , with  $c_p$  and  $c_T$  are velocities of the longitudinal and transverse waves, respectively. We consider a division into time and space that respects the condition

$$\frac{\varepsilon_1}{\delta} = \frac{\varepsilon_2}{\delta} \geq \sqrt{v_l^2 + v_t^2}. \quad (29)$$

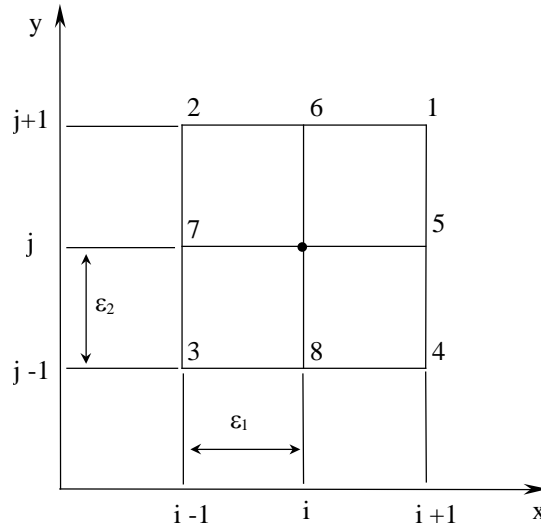


Fig.1. Nodes.

The numerical stability analysis of recurrence equations is done by using the Von Nemann method which consists in replacing of the discrete displacements in the recurrence equations with Fourier transform. In the two-dimensional case we have

$$w_{i,j,t} \rightarrow w_0 e^{i(mx+ny)} g^t, \quad (30)$$

where  $x = i\varepsilon_1$ ,  $y = j\varepsilon_2$ . Introducând (30) în (28) se obține

$$\begin{bmatrix} 2D_1 - g - g^{-1} & -\sqrt{D_3} \\ -\sqrt{D_3} & 2D_2 - g - g^{-1} \end{bmatrix} \cdot \begin{bmatrix} u \\ v \end{bmatrix} = \begin{bmatrix} 0 \\ 0 \end{bmatrix}, \quad (31)$$

where

$$\begin{aligned} D_1 &= 1 - 2c^2(d + abe), \\ D_2 &= 1 - 2c^2(bd + ac), \\ D_3 &= 16(1-b)^2 ac^4 de(1-d)(1-e), \end{aligned} \quad (32)$$

$$a = \left( \frac{\varepsilon_1}{\varepsilon_2} \right)^2, \quad b = \left( \frac{c_T}{c_L} \right)^2, \quad c = c_L \frac{\delta}{\varepsilon_1}, \quad d = \sin^2 \frac{m\varepsilon_1}{2}, \quad e = \sin^2 \frac{n\varepsilon_2}{2}.$$

In order that (31) to admit solutions, the determinant of the system (31) must be null

$$(g^2 - 2D_1g + 1)(g^2 - 2D_2g + 1) - D_3g^2 = 0, \quad (33)$$

or

$$(g^2 - 2A_1g + 1)(g^2 - 2A_2g + 1) = 0, \quad (34)$$

where

$$A_1 = \frac{1}{2} \left( D_1 + D_2 + \sqrt{(D_1 - D_2)^2 + D_3} \right) = 1 - c^2(1+b)(d + ae) + c^2(1-b)\sqrt{s}, \quad (35)$$

$$A_2 = \frac{1}{2} \left( D_1 + D_2 - \sqrt{(D_1 - D_2)^2 + D_3} \right) = 1 - c^2(1+b)(d + ae) - c^2(1-b)\sqrt{s}, \quad (36)$$

with

$$s = (d - ae)^2 + 4ade(1-d)(1-e). \quad (37)$$

The numerical stability testing of equations with finite differences imposes  $|g| \leq 1$ , from which it results  $|A_1| \leq 1$  and  $|A_2| \leq 1$ . From (35), the condition  $|A_1| \leq 1$  becomes

$$-1 \leq 1 - c^2(1+b)(d + ae) + c^2(1-b)\sqrt{s} \leq 1, \quad (38)$$

equivalent to

$$0 \leq c^2(1+b)(d + ae) - c^2(1-b)\sqrt{s} \leq 2. \quad (39)$$

From (36), the condition  $|A_2| \leq 1$  gives

$$-1 \leq 1 - c^2(1+b)(d + ae) - c^2(1-b)\sqrt{s} \leq 1. \quad (40)$$

equivalent to

$$0 \leq c^2(1+b)(d + ae) + c^2(1-b)\sqrt{s} \leq 2. \quad (41)$$

Because  $0 \leq d \leq 1$ ,  $0 \leq e \leq 1$ ,  $0 \leq b \leq 1$ ,  $0 \leq a$  and  $0 \leq c$ , the right side of (39) and (41) is verified.

The approximation  $\sqrt{s} \geq |d - a \cdot e|$  gives

$$c^2(1+b)(d + ae) - c^2(1-b)\sqrt{s} \leq c^2(1+b)(d + ae) - c^2(1-b)|d - ae|. \quad (42)$$

The inequality on the right side of the relationship (41), taking into account (42), becomes

$$c^2 \leq \frac{2}{(1+b)(d+ae)-(1-b)|d-ae|} = \begin{cases} \frac{1}{d+abe} & \text{if } d \leq ae, \\ \frac{1}{bd+ae} & \text{if } d \geq ae, \end{cases} \quad (43)$$

In the worst case  $d = e = 1$ , (43) becomes

$$c^2 \leq \min \left[ \frac{1}{1+ab}, \frac{1}{a+b} \right] = \begin{cases} \frac{1}{1+ab}, & a \leq 1, \\ \frac{1}{b+a}, & a \geq 1, \end{cases} \quad (44)$$

From

$$\sqrt{s} \leq \begin{cases} d+ae-2ade, & a \leq 1 \\ d+ae-2de, & a \geq 1 \end{cases} \quad (45)$$

we have

$$c^2(1+b)(d+ae) + c^2(1-b)\sqrt{s} \leq \begin{cases} c^2(1+b)(d+ae) + \\ + c^2(1-b)(d+ae-2ade) & a \leq 1 \\ c^2(1+b)(d+ae) + \\ + c^2(1-b)(d+ae-2de) & a \geq 1 \end{cases} \quad (46)$$

Taking into account (46), inequality on the right side of the relationship (41) becomes

$$c^2 \leq \begin{cases} \frac{1}{ae+d(1-(1-b)ae)}, & a \leq 1, \\ \frac{1}{ae+d(1-(1-b)e)}, & a \geq 1, \end{cases} \quad (47)$$

In the worst case  $d = e = 1$ , (47) is identical with (44).

So, the relationship of stability is

$$c_p \delta \leq \begin{cases} \varepsilon_1 \frac{1}{\sqrt{1 + \frac{c_T^2 \varepsilon_1^2}{c_L^2 \varepsilon_2^2}}} & \text{if } \frac{\varepsilon_1}{\varepsilon_2} \leq 1, \\ \varepsilon_2 \frac{1}{\sqrt{1 + \frac{c_T^2 \varepsilon_1^2}{c_L^2 \varepsilon_2^2}}} & \text{if } \frac{\varepsilon_1}{\varepsilon_2} \geq 1, \end{cases} \quad (48)$$

which reduces, for a uniform meshing, to (29).

To extend recurrence relations in the interfaces, it is assumed that the properties of the material are constant in the cell. We consider the point at the intersection of four mediums with different properties  $\rho_k, \lambda_k, \mu_k, R_k$ ,  $k = 1, 2, 3, 4$  (Fig. 2). The points  $P_k$  have location  $(i \pm \eta, j \pm \eta)$ .

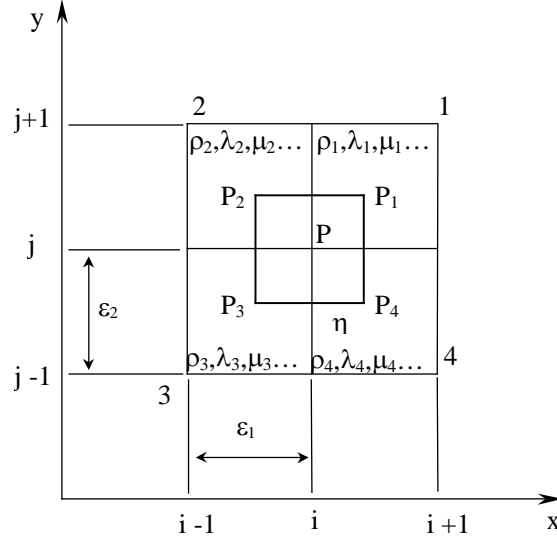


Fig. 2. The intersection point of four adjacent media.

We impose the condition of continuity of the temporal derivations of the displacements so that for  $\eta \rightarrow 0$ , to have  $\ddot{W}_{P_k} \approx \Omega$ . This condition is ensured by the continuity of displacements at the initial moments. Since within the cell the material is homogeneous, we calculate  $W_{,kh}$ ,  $k, h = 1, 2$  from (23). Using the finite differences we have

$$\begin{aligned} \rho_1 \Omega \approx & 2A_1 \frac{W_{1,1}}{\varepsilon_1} - 2B_1 \frac{W_{1,2}}{\varepsilon_2} + \\ & + \left( 2A_1 \frac{(W_5 - W)}{\varepsilon_1^2} + 2B_1 \frac{(W_6 - W)}{\varepsilon_2^2} + C_1 \frac{(W_1 + W - W_5 - W_6)}{\varepsilon_1 \varepsilon_2} \right) \end{aligned} \quad (49)$$

$$\begin{aligned} \rho_2 \Omega \approx & 2A_2 \frac{W_{2,1}}{\varepsilon_1} - 2B_2 \frac{W_{2,2}}{\varepsilon_2} + \\ & + \left( 2A_2 \frac{(W_7 - W)}{\varepsilon_1^2} + 2B_2 \frac{(W_6 - W)}{\varepsilon_2^2} + C_2 \frac{(W_6 + W_7 - W - W_2)}{\varepsilon_1 \varepsilon_2} \right) \end{aligned} \quad (50)$$

$$\begin{aligned} \rho_3 \Omega \approx & 2A_3 \frac{W_{3,1}}{\varepsilon_1} + 2B_3 \frac{W_{3,2}}{\varepsilon_2} + \\ & + \left( 2A_3 \frac{(W_7 - W)}{\varepsilon_1^2} + 2B_3 \frac{(W_8 - W)}{\varepsilon_2^2} + C_3 \frac{(W + W_3 - W_7 - W_8)}{\varepsilon_1 \varepsilon_2} \right) \end{aligned} \quad (51)$$

$$\begin{aligned} \rho_4 \Omega \approx & 2A_4 \frac{W_{4,1}}{\varepsilon_1} - 2B_4 \frac{W_{4,2}}{\varepsilon_2} + \\ & + \left( 2A_4 \frac{(W_5 - W)}{\varepsilon_1^2} + 2B_4 \frac{(W_8 - W)}{\varepsilon_2^2} + C_4 \frac{(W_5 + W_8 - W - W_4)}{\varepsilon_1 \varepsilon_2} \right) \end{aligned} \quad (52)$$

where  $W$  is the displacement vector in point  $P$ ,  $W_n$  is the displacement vector in points  $n = 1, 2, \dots, 8$  (Fig. 1).  $A_k$ ,  $B_k$  and  $C_k$  correspond to four media.

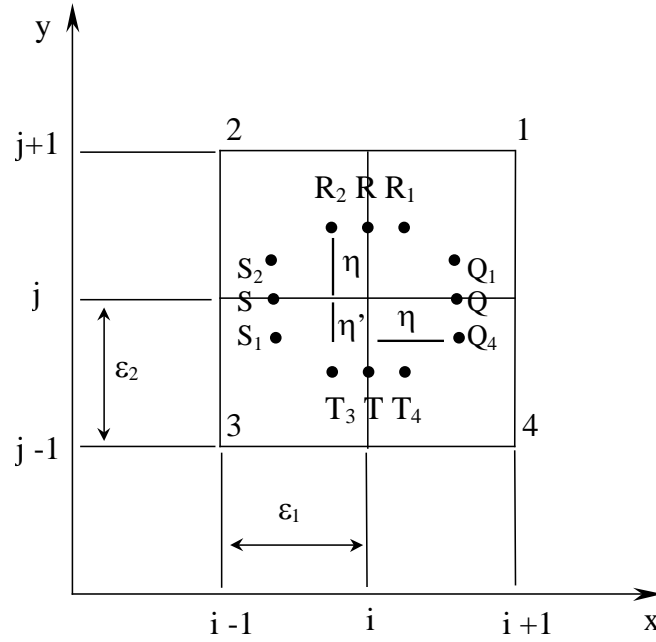


Fig. 3 Representation of points for continuity conditions.

We consider four points  $Q$ ,  $R$ ,  $S$  and  $T$  at the distance  $\eta \ll \varepsilon$  from  $P$ , and eight points  $Q_4$ ,  $Q_1$ ,  $R_1$ ,  $R_2$ ,  $S_2$ ,  $S_3$ ,  $T_3$ ,  $T_4$  at the distance  $\eta' \ll \eta$  from  $Q$ ,  $R$ ,  $S$  and  $T$ , respectively (Fig. 3).

We impose the continuity conditions of tensions in  $P$

$$(\tau_1)_{R_2} = (\tau_1)_{R_1}, \quad (\tau_1)_{T_3} = (\tau_1)_{T_4} \quad (53)$$

$$(\tau_1)_{T_3} = (\tau_1)_{T_4}, \quad (\tau_2)_{S_3} = (\tau_2)_{S_2} \quad (54)$$

The constitutive law for isotropic environments results

$$\tau_1 = AW_{,1} + DW_{,2}, \quad (55)$$

$$\tau_2 = EW_{,1} + BW_{,2}, \quad (56)$$

### 3. APPLICATIONS

Consider the one-dimensional wave propagation in a three-dimensional jointed plate shown in Fig. 4. [8-12]. The plate occupies the region  $x \in [a, b]$ ,  $|y| < \infty$ , and  $|z| < \infty$  consisting of a nonhomogeneous matrix material subdivided by periodically spaced joints. The joints are parallel, planar, periodically spaced surfaces of zero thickness, across which the displacements are allowed to be discontinuous. The joints are located at  $2nh$ ,  $2(n+1)h$ ,  $2(n+2)h$  and so on,  $n \in \mathbb{Z}$ , each joint having two faces identified by  $+$  and  $-$ . Now let  $b-a$  be small, but large enough that the interval  $[a, b]$  contains many joints. Choose coordinates so that the waves lie in the  $(x, z)$  plane. The plate is assumed to be in plane strain and to support waves running in the  $x$ -direction. A finite duration  $P$  or  $S$  pulse, with wavelength much larger than the cell dimension  $2h$ , propagates obliquely through the plate on the face  $x = a$ .

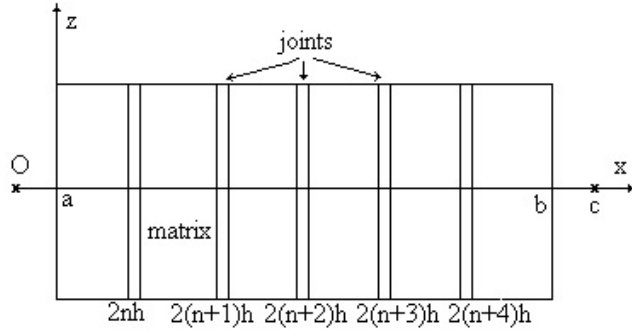


Fig. 4. Jointed medium.

The motion equations for the displacement field  $u(x, z, t)$  and the stress field  $\sigma(x, z, t)$  are [8, 11]

$$\sigma_{ij,j} = \rho \ddot{u}_i, \quad i = 1, 3, \quad (57)$$

$$\varepsilon_{ij} = \frac{1}{2}(u_{i,j} + u_{j,i}), \quad \sigma_{ij} = \lambda \varepsilon_{kk} \delta_{ij} + 2\mu \varepsilon_{ij}, \quad i, j = 1, 2, 3, \quad (58)$$

$$\sigma_{11}(2nh^-, t) = \sigma_{11}(2nh^+, t), \quad \sigma_{13}(2nh^-, t) = \sigma_{13}(2nh^+, t), \quad (59)$$

$$\sigma_{ij}(2nh^-, t) = D_{ij}[u_1(2nh^+, t) - u_1(2nh^-, t)], \quad (60)$$

$$u_i = \sigma_{ij} = 0, \quad i, j = 1, 3, \quad y, z \rightarrow \pm\infty, \quad (61)$$

where the comma means differentiation with respect to the variable  $x_i$  ( $x_1 \equiv x$ ,  $x_2 \equiv y$ ,  $x_3 \equiv z$ ), the dot differentiation with respect to time and  $\rho$  is the material density,  $\lambda(x)$  and  $\mu(x)$  are the Lamé moduli for the matrix,  $D_{11} = \lambda_0 + 2\mu_0$ ,  $D_{13} = \mu_0$  and  $D_{33} = \lambda_0$ , where  $\lambda_0, \mu_0$  are the elastic moduli for the joint.

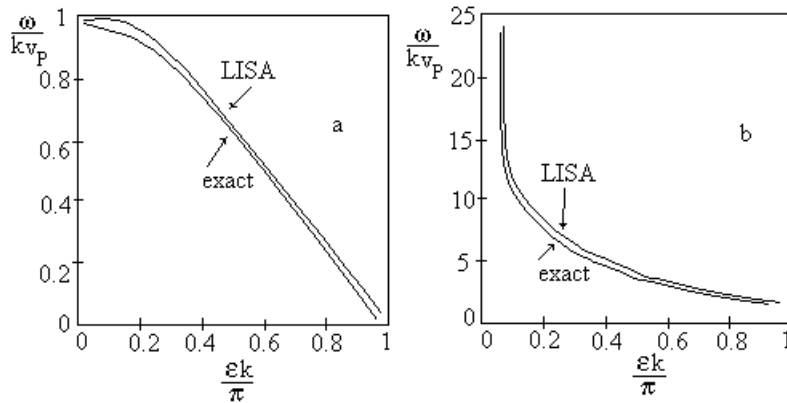


Fig. 5. Dispersion curves for a) acoustic mode and b) the first optical mode

The relations (59) are verified by all the joints. Non-vanishing displacements are  $u_1$  and  $u_2$ . Conditions (59) and (60) represent stress continuity for the joint  $2nh$  for  $|z| < \infty$ , and joint constitutive law for the joint  $2nh$ , respectively. Relation (61) is the radiation condition.

To test the efficacy of the LISA method we consider first the simple case when  $u_3 = 0$  and  $\lambda(x) = \lambda$  and  $\mu(x) = \mu$ . The exact dispersion relation for harmonic-wave propagation is obtained by assuming solutions of the form  $u(x, t) = U(x) \exp(i(kx - \omega t))$ .

The equations (57)-(61) lead to the dispersion relation calculated in [11]

$$\varepsilon k h \frac{\omega}{k v_p} \sin\left(2\varepsilon k h \frac{\omega}{k v_p}\right) = 4 \frac{D_{11} h}{\lambda + 2\mu} \sin\left(2\varepsilon k h \left(1 + \frac{\omega}{k v_p}\right)\right) \sin\left(2\varepsilon k h \left(1 - \frac{\omega}{k v_p}\right)\right), \quad (62)$$

In Fig. 5 we compare the results for the dispersion of the acoustic mode for  $\frac{\lambda + 2\mu}{D_{11} h} = 10$ , and

in Fig. 5b the results for the dispersion of the lowest optical mode on LISA model with the exact solution. Evidently, LISA provides a highly accurate model of dispersion. We mention, also, the agreement of LISA results with the results given by using the homogenised model developed in [8, 11]. Next, we apply LISA to the case of a plane  $P$  wave incident at  $\theta = 15^\circ$  as it traverses a plate of 10, 20, 40 and 60 joints. The pulse is gaussian.

In Fig. 6 this pulse measured in the observer  $x = c$  is represented after travelling a number of 10-55 joints. We observe the progressive broadening of the pulse in perfect agreement with the results in [10]. The calculus was performed for  $\bar{\rho} = 2700 \text{ kg/m}^3$ ,  $\bar{v}_s = 30080 \text{ m/s}$ ,  $\bar{v}_p = 6260 \text{ m/s}$  and for each cell  $J = 1, 2, \dots, N$  we have taken  $\rho(J) = \bar{\rho} + \delta$ ,  $v_s(J) = \bar{v}_s + \delta$ ,  $v_p(J) = \bar{v}_p + \delta$  with a random  $\delta \in [-20, 20]$ . For joints we have taken  $\lambda + 2\mu = 10D_{11}h$ ,  $\mu = 10D_{13}h$  and  $\lambda = 10D_{33}h$ .

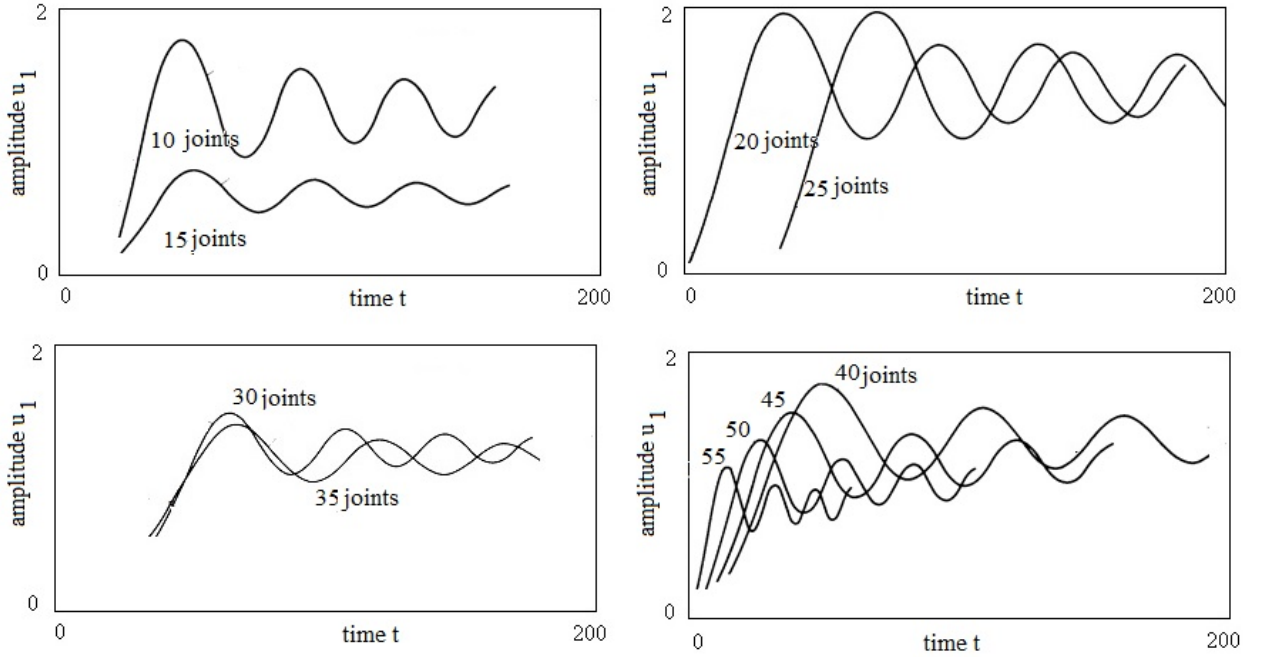


Fig. 6. P impulse incident at  $\theta = 15^\circ$  after traveling through 10-55 joints.

#### 4. CONCLUSIONS

This paper applies the local interaction simulation approach (LISA) for simulation of wave propagation in a layered plate. Delsanto et al. [1, 2] have introduced this method for simulation the propagation of ultrasonic wave in layered materials. The layered material is discretized in cells, each cell being associated to a layer with different mechanical properties. Each cell is put into a

one-to-one correspondence to a processor of a parallel computer. The material properties are assigned as initial data to each processor. LISA aims to teach processors how the corresponding cells react to the arriving wave and propagate it to the neighbors by using a special interaction mechanism. LISA is efficient and flexible, especially in conjunction with parallel processing. The method is applied to study the ultrasonic wave propagation in materials of arbitrary complexity and to solve some inverse problems of their characterization.

Received on September 28, 2017

## REFERENCES

1. DELSANTO, P.P., WHITCOMBE, T., CHASKELIS, H.H., MIGNOGNA, R.B., *Connection machine simulation of ultrasonic wave propagation in materials, I: the one-dimensional case*, Wave Motion 16, 1992.
2. DELSANTO, P.P., SCHECHTER, R.S., CHASKELIS, H.H., MIGNOGNA, R.B., KLINE, R., *Connection machine simulation of ultrasonic wave propagation in materials, II: the two-dimensional case*, Wave Motion 20, 1994.
3. DELSANTO, P.P., WHITCOMBE, T., CHASKELIS, H.H., MIGNOGNA, R.B., *Use of the connection machine to study ultrasonic wave propagation in materials*, in D.O.Thompson and D.E.Chimenti, eds., Proc. 16th Annual Review of Progress in QNDE, 9A, Plenum, 1990.
4. DELSANTO, P.P., WHITCOMBE, T., BATRA, N.K., CHASKELIS, H.H., MIGNOGNA, R.B., *Connection machine simulation of the ultrasonic wave propagation in attenuative materials*, in D.O.Thompson and D.E.Chimenti, eds., Proc. 17th Annual Review of Progress in QNDE, 10A, Plenum, 1991.
5. DELSANTO, P.P., WHITCOMBE, T., CHASKELIS, H.H., MIGNOGNA, R.B., *Connection machinesimulation of ultrasonic wave propagation: two dimensional case*, in D.O.Thompson and D.E.Chimenti, eds., Proc. 18<sup>th</sup> Annual Review of Progress in QNDE, 11A, Plenum, 1992.
8. CHIROIU, V., IORDACHE, D., SCALERANDI, M., CHIROIU, C., *Simulation of ultrasonic wave propagation in thin composite plates by means of LISA*, Rev. Roum. Sci.Tech.- Mec.Appl., Tome 43, No 6 , p.675-684, Bucurest,1998.
9. CHIROIU, V. CHIROIU, C., *Probleme inverse în mecanică*, Editura Academiei, Bucharest, 2003.
10. BURRIDGE, R., HUNG-WEN CHANG, *Pulse evolution in a multimode, one-dimensional, highly discontinuous medium*, Elastic Wave Propagation, M.F. McCarthy, M.A. Hayes, eds., Elsevier Science Publishers B.V., North-Holland 1989.
11. SHKOLLER, S., MAEWAL, A., HEGEMIER, G.A., *A dispersive continuum model of jointed media*, Quarterly of Applied Mathematics, LII, 1994.
12. DELSANTO, P.P., MUNTEANU, L., CHIROIU, V., DONESCU, Ș.T., *On the nanotorsional pendulum*, Proceedings of the Romanian Academy, Series A: Mathematics, Physics, Technical Sciences, Information Science, 10(2), 173-178, 2009.